Remote Sensing of Environment 191 (2017) 168–178

Contents lists available at ScienceDirect

Remote Sensing of Environment

journal homepage: www.elsevier.com/locate/rse

Characterizing global patterns of frozen ground with and without snow cover using microwave and MODIS satellite data products

Likai Zhu [a,*], Volker C. Radeloff [a], Anthony R. Ives [b]

[a] SILVIS Lab, Department of Forest and Wildlife Ecology, University of Wisconsin-Madison, 1630 Linden Drive, Madison, WI 53706, USA
[b] Department of Zoology, University of Wisconsin-Madison, 250 N. Mills Street, Madison, WI 53706, USA

ARTICLE INFO

Article history:
Received 31 August 2016
Received in revised form 12 December 2016
Accepted 18 January 2017

Keywords:
MODIS
MEaSUREs Freeze/Thaw data records
Snow cover
Frozen ground
Frozen season
Subnivium

ABSTRACT

How organisms respond to climate change during the winter depends on snow cover, because the subnivium (the insulated and thermally stable area between snowpack and frozen ground) provides a refuge for plants, animals, and microbes. Satellite data characterizing either freeze/thaw cycles or snow cover are both available, but these two types of data have not yet been combined to map the subnivium. Here, we characterized global patterns of frozen ground with and without snow cover to provide a baseline to assess the effects of future winter climate change on organisms that depend on the subnivium. We analyzed two remote sensing datasets: the MODIS Snow Cover product and the NASA MEaSUREs Global Record of Daily Landscape Freeze/Thaw Status dataset derived from SSM/I and SSMIS. From these we developed a new 500-m resolution dataset that captures global patterns of the duration of snow-covered ground (D_{ws}) and the duration of snow-free frozen ground (D_{wos}) from 2000 to 2012. We also quantified how D_{ws} and D_{wos} vary with latitude. Our results show that both mean and interannual variation in D_{ws} and D_{wos} change with latitude and topography. Mean D_{ws} increases with latitude. Counter-intuitively though, D_{wos} has longest duration at about 33°N, decreasing both northward and southward, even though the duration of frozen ground (either snow covered or not) was shorter than that at higher latitudes. This occurs because snow cover in mid-latitudes is low and ephemeral, leaving longer periods of frozen, snow-free ground. Interannual variation in D_{ws} increased with latitude, but the slopes of this relationship differed among North America, Europe, Asia, and the Southern Hemisphere. Overall, our results show that, for organisms that rely on the subnivium to survive the winter, mid-latitude areas could be functionally colder than either higher or lower latitudes. Furthermore, because interannual variation in D_{wos} is greater at high latitudes, we would expect organisms there to be adapted to unpredictability in exposure to freezing. Ultimately, the effects of climate change on organisms during winter should be considered in the context of the subnivium, when warming could make more northerly areas functionally colder in winter, and changes in annual variation in the duration of snow-free but frozen conditions could lead to greater unpredictability in the onset and end of winter.

1. Introduction

Winter is a key driver of species distributions through its effects on individual performance, community composition, and ecological interactions (Williams et al., 2014). Thus, differences in the distributions of species often reflect differences in their susceptibility to resource scarcity and energy deficits during winter (Kreyling, 2010; Pauli et al., 2013). Discussions of the effects of climate change on ecological systems are often centered around the growing season, where climate warming will affect flowering phenology, the length of the growing season, droughts, fire regimes, etc. However, winter is also subject to climate change (Williams et al., 2014) through changes in snow cover, soil freeze/thaw cycles, and lake and river ice (Fountain et al., 2012; Kim et al., 2012; Peng et al., 2013). These changes may strongly influence biophysical conditions and biogeochemical processes (Fountain et al., 2012; Makoto et al., 2013), and hence organisms (Kreyling, 2010; Pauli et al., 2013). Winter as a distinct season attracts less scientific attention by biologists than other seasons, at least partly due to the perception that there is little biological activity and to the inherent difficulties of field work during winter (Campbell et al., 2005).

Whether or not an area is covered by snow during winter can greatly affect the condition and survival of organisms because snow cover affects microclimates (Decker et al., 2001; Isard and Schaetzl, 2007; Williams et al., 2014). Beneath the snow there is an insulated and thermally stable refugium – the subnivium (Pauli et al., 2013). The subnivium forms when heat is released from the soil, and warm, moist air is trapped by the snow (Petty et al., 2015). Areas with a

* Corresponding author.
E-mail address: lzhu68@wisc.edu (L. Zhu).

http://dx.doi.org/10.1016/j.rse.2017.01.020
0034-4257/

subnivium generally have higher overwintering success of plants, animals, and microbes (Aitchison, 2001; Pauli et al., 2013; Williams et al., 2014). The higher temperatures in the subnivium can reduce root damage and plant death during winter by alleviating frost penetration into the soil (Kreyling, 2010; Starr and Oberbauer, 2003). Animals that overwinter in surface soils, including reptiles, amphibians and insects, may require the thermally stable subnivium for survival (Aitchison, 2001; Bale and Hayward, 2010; Jones, 1999; Williams et al., 2014). Furthermore, the subnivium can also keep soil temperatures above the threshold required for microbial respiration (Pauli et al., 2013; Sullivan et al., 2008), causing rates of soil microbial activity to be sufficiently high in winter to comprise a significant percentage of annual activity (Campbell et al., 2005). High rates of microbial activity can also result in increased mineralization of organic matter and trace gas concentrations during winter (Campbell et al., 2005; Pauli et al., 2013; Schimel et al., 2004). However, despite its ecological importance, the subnivium has not been mapped globally (Pauli et al., 2013; Williams et al., 2014).

Mapping the subnivium requires information on frozen ground and snow cover, yet most research has focused on only one of these two attributes. As a result, there are excellent remote sensing datasets of freeze/thaw cycles in terms of the date of spring thaw, the date of fall freeze, and the duration of the frozen/non-frozen season (Kim et al., 2012; Smith et al., 2004; Zhang et al., 2011), as well as assessments how these dates have shifted in recent decades, causing earlier spring thaw and shorter frozen seasons. Similarly, there are excellent remote sensing datasets of the length of the snow season, the maximum snow depth, the maximum snow extent, the timing of snowmelt, etc. (Déry and Brown, 2007; Dye, 2002; Kim et al., 2015; Peng et al., 2013). Trends in recent decades have been earlier spring snowmelt, longer snowmelt periods, and decreased snow cover duration (Kim et al., 2015; Peng et al., 2013). However, to our knowledge, few studies have combined freeze/thaw status and snow cover (Kim et al., 2015), even though the combination of these two attributes determines the duration of the subnivium.

Satellite remote sensing data have greatly advanced the scientific understanding of snow cover, soil freeze/thaw status, and other winter-specific variables at regional to global scales. Ground-based meteorological networks have been monitoring snow for a long time, but the discrete distribution of stations cannot capture spatial variability, especially in remote areas (Pu et al., 2007). A number of digital snow products based on remote sensing observations are available (Frei et al., 2012), and the longest NOAA snow cover extent (SCE) climate record (CDR) has been widely used for regional-scale climate studies, monitoring, and model validation (Estilow et al., 2014). A suite of MODIS snow cover products available since 2000 have been generated using MODIS sensor measurements (Hall et al., 2002). The advantage of the MODIS data is their higher spatial resolution. In particular, the 8-day composite product of MOD10A2 minimizes the effect of cloud contamination (Liang et al., 2008), and its global availability at 500-m resolution is ideal for broad-scale research on winter ecology.

Microwave remote sensing is well suited for freeze/thaw monitoring due to its relative insensitivity to atmospheric contamination and solar illumination effects, and strong sensitivity to changes in the predominant frozen/thawed state of water (Kim et al., 2011; Kim et al., 2012). One of the NASA MEaSUREs Global Record of Daily Landscape Freeze/Thaw Status datasets from Scanning Multichannel Microwave Radiometer (SMMR), Special Sensor Microwave/Imager (SSM/I), and Special Sensor Microwave Imager/Sounder (SSMIS) provides a consistent long-term global record available daily since 1979 of land surface freeze/thaw state dynamics for all vegetated regions where low temperatures are a major constraint on ecosystem processes. Prior analyses of this dataset have revealed close biophysical linkages between several freeze/thaw-associated variables and the duration of seasonal snow and frozen ground, the timing and length of the growing season, and vegetative productivity and water cycling (Kim et al., 2012, 2015; Zhang et al., 2011). The microwave satellite-based dataset is thus an ideal option for monitoring ground freeze/thaw status given its long duration.

Here, we characterize global patterns of frozen ground with and without snow cover to assess the duration of the subnivium; this provides baseline data to understand current and forecast future winter conditions that affect overwintering organisms. We combined two datasets, the MODIS Snow Cover product and the NASA MEaSUREs Freeze/Thaw dataset from SSM/I and SSMIS, and developed a new 500-m resolution dataset from 2000 to 2012 which shows global patterns of the duration of snow-covered ground (D_{ws}) and the duration of snow-free frozen ground (D_{wos}). We defined the timing and length of the frozen season based on the daily freeze/thaw records. To illustrate the potential use of our new dataset, we investigated latitudinal patterns in the mean and variation of D_{ws} and D_{wos}. These patterns show both nonlinear latitudinal gradients and differences in latitudinal gradients among continents, emphasizing the value of our dataset.

2. Data and methods

2.1. Data

We used the NASA MEaSUREs Global Record of Daily Landscape Freeze/Thaw Status dataset (Version 3) from SSM/I and SSMIS to determine frozen/thawed status, and the timing and duration of the frozen season. The dataset is available on a daily basis with 25-km spatial resolution from 1979 to 2012. It applies a seasonal threshold approach to the continuous daily (A.M. and P.M.) radiometric brightness temperatures (Kim et al., 2011). Thus, four discrete categories are distinguished on a daily basis: frozen (A.M. and P.M.), thawed (A.M. and P.M.), transitional (A.M. frozen and P.M. thawed), and inverse transitional (A.M. thawed and P.M. frozen) ground. Mean annual classification accuracies at P.M. and A.M. are approximately 92.2 and 85.0%, respectively (Kim et al., 2011). The retrieved status represented predominant frozen or thawed conditions within the satellite footprint and does not distinguish individual landscape elements, including soil, vegetation, and snow cover (Kim et al., 2015). The dataset excludes non-vegetated areas, and those areas which are not constrained by seasonal cold temperatures detected by a simple cold temperature constraint index (Kim et al., 2015). The daily dataset is available at the National Snow & Ice Data Center (NSIDC) (http://nsidc.org/).

We analyzed the 8-day composite MODIS Snow Cover product (MOD10A2) to determine ground snow-cover status. The dataset is available globally, at a spatial resolution of 500 m, from 2000 to present. The snow-cover algorithm is based on a grouped-criteria technique, which applies band ratio and a suite of threshold-based criteria to determine snow or no snow status on different land-cover types (Hall et al., 2002). The MODIS snow cover products have been assessed at both global and regional scales, and the overall accuracy is generally >80% but varies by land-cover type, snow conditions (e.g., snow depth), and the number of days used to make the composite (Hall and Riggs, 2007; Klein and Barnett, 2003; Liang et al., 2008; Pu et al., 2007). Compared to the daily MODIS snow cover product (MOD10A1), the 8-day composite effectively reduces cloud contamination and thereby provides more consistent coverage (Liang et al., 2008; Pu et al., 2007). Because MODIS sensors cannot receive optical information effectively in high-latitude areas during winter due to the effect of polar night, we were not able to analyze areas above 62°N. The MODIS snow cover data that we used were also downloaded from the NSIDC.

2.2. Methods

We defined the timing and duration of the frozen season annually on a pixel basis, and calculated D_{ws} and D_{wos} within the pre-defined frozen season (Fig. 1). For each pixel, we calculated the freeze frequency, which we defined as the number of occurrences of frozen ground (A.M. and P.M. frozen, A.M. frozen and P.M. thawed) at the same day-of-year

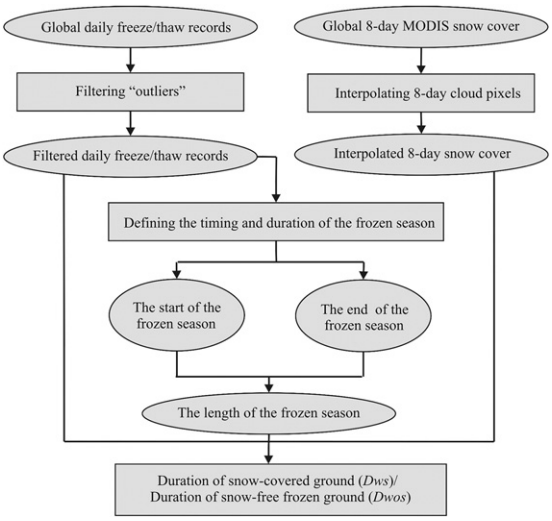

Fig. 1. Flowchart of the major data processing procedures to assess the duration of snow-covered ground, and snow-free frozen ground.

(DOY) during the 13 years (2000−2012); as an example for a single calendar day, we gave the frequency map at DOY 210 (Fig. S1). We found that there were some pixels with frozen or transitional status occurring only one time (frequency = 1) during the 13 years, especially during the summertime; for example, in DOY210 singleton pixels occurred at middle or low latitudes in the northern hemisphere (Fig. S2). We treated these pixels with caution by examining their neighborhoods within specific spatial and temporal windows, respectively. For each pixel with frequency equal to 1, we checked the freeze/thaw status of its six adjacent dates in the year that frozen ground appeared in the data, and its eight neighboring pixels within a 3 by 3 pixel window. If the occurrence of frozen ground was equal to or greater than one within neighboring pixels in either time or space, then we left the frozen pixel unchanged. If not, we treated the frozen pixel for the specific year as an "outlier" and reclassified it as thawed status. On average, the number of pixels with a freeze frequency equal to 1 was 52,749 per year, and out of these we did not incorporate into our subsequent analyses on average 11,274 per year for the full year, and 2010 per year for the frozen season (Fig. S3). Because the number of pixels that we removed (2011 per frozen season) accounted for very small proportion of total frozen pixels (12,744,067 per frozen season on average), this step did not affect our general conclusions, but it removed likely erroneous observations. Through these steps, we derived a filtered daily freeze/thaw dataset with "outliers" removed.

Even though the 8-day composite MODIS Snow Cover product effectively reduced cloud cover, there were still some cloud pixels which would cause underestimates of D_{ws}. Thus, we interpolated the cloud pixels within the 8-day composite snow-cover images in winter months (Northern Hemisphere: December–February; Southern Hemisphere: June–August). For a given cloud pixel, we examined the snow cover status of its four neighboring pixels (sharing an edge) and its two adjacent MODIS dates. Spatially, if all four neighboring pixels were classified as snow, we treated the central cloud pixel as snow. If the above criterion was not met but temporally the pixels at the two adjacent MODIS dates were both classified as snow, then we also reclassified the cloud pixel as snow. If both criteria were not met, then we treated the cloud pixel as no snow cover. We derived a new 8-day snow cover dataset with interpolated cloud pixels if the above criteria were met.

We determined the timing and length of the frozen season annually for each pixel using the daily freeze/thaw records so that we confined our analysis within the prevalent frozen period. We defined the start and end of the frozen season according to prior non-frozen season definitions (Kim et al., 2012; Xu et al., 2013; Zhang et al., 2011). For the Northern Hemisphere, the start of the frozen season was defined as the middle day of the first period of 15 consecutive days from September through February for which at least 8 days were classified as frozen (including A.M. and P.M. frozen, and A.M. frozen and P.M. thawed). The end of the frozen season was determined as the middle day of the first period of 15 consecutive days from February to August for which at least 8 days were classified as thawed (A.M. and P.M. thawed). For the Southern Hemisphere, we examined the periods March–August and September–February to identify the start and end of the frozen season, respectively. If there was no frozen or transitional status detected in any year for a specific pixel, we defined it as "no frozen days". If neither a start nor an end of the frozen season was detected in any year for a specific pixel, we defined it as "no frozen season". The length of the frozen season was defined as the period between the start and end of the frozen season. We calculated the start and end of the frozen season globally for each year from 2000 to 2012, and used them to constrain our calculations of D_{ws} and D_{wos} within the range of the frozen season.

We calculated D_{ws} and D_{wos} annually for each pixel by integrating the freeze/thaw status, the snow-cover status, and the range of the frozen season. If a pixel had both frozen ground and snow cover, and its date was within the range of the frozen season, one day was added to

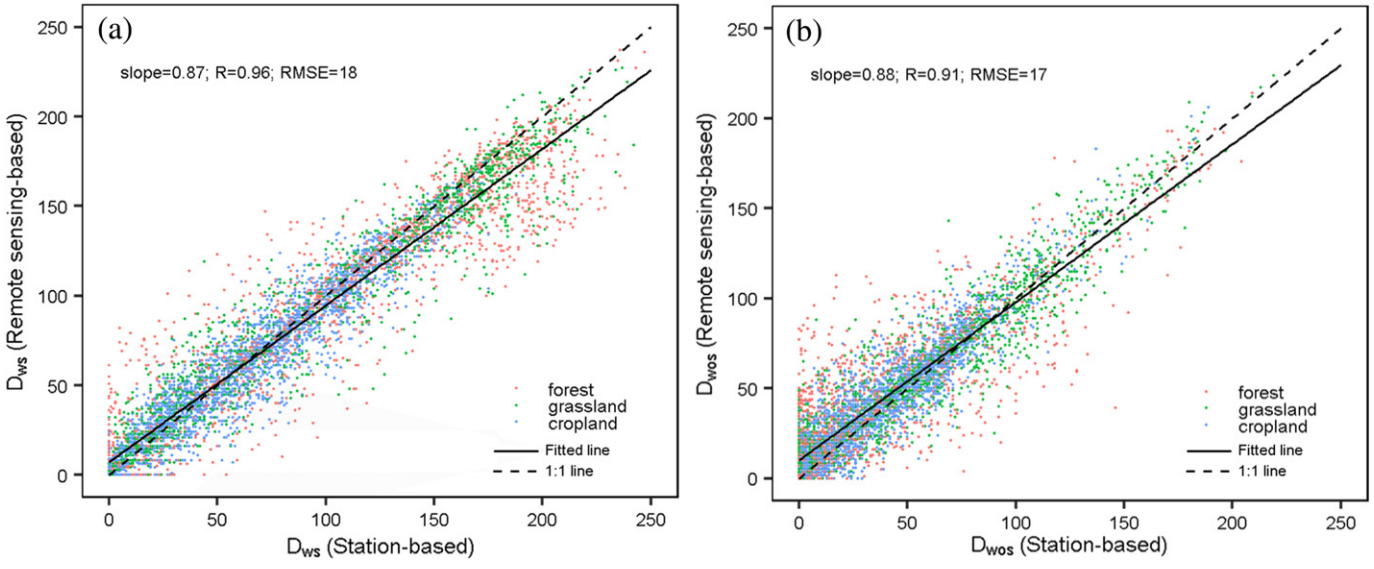

Fig. 2. Scatterplots (a) between station-based D_{ws} and remote sensing-based D_{ws}, and (b) between station-based D_{wos} and remote sensing-based D_{wos}.

Table 1
Correlation coefficients, linear regression slopes, and root-mean-square errors between station-based D_{ws} and remote sensing-based D_{ws} by land cover classes and elevation levels.

	Land cover class			Elevation			
	Forest	Grassland	Cropland	<=250 m	250– 500 m	500– 1500 m	>1500 m
R	0.94	0.97	0.96	0.93	0.94	0.94	0.94
Slope	0.83	0.89	0.93	0.82	0.87	0.88	0.82
RMSE	24	17	13	18	15	17	21

D_{ws}. Likewise, if a pixel was classified as frozen ground without snow cover, and its date was within the range of the frozen season, then one day was added to D_{wos}. Because we combined the datasets with different spatial resolutions, our calculations assumed that the frozen status was homogeneous within a 25-km pixel. To test the validity of this assumption, we analyzed Daymet daily minimum temperature data for North America at 1-km spatial resolution from 2000 to 2012 (Thornton et al., 2016), and calculated the percentage pixels whose minimum temperature was <0 °C within the corresponding frozen pixel at 25-km resolution at the same date. We summarized the percentages by the days of year and by frozen seasons (Fig. S4 and Fig. S5). The percentages from DOY 1 to 150, and DOY 270 to 365 were stable and high, and the average percentage was about 97% (Fig. S4). The percentages decreased after DOY150, and then increased after reaching the minimum at about DOY 200. However, the period with low and unstable percentages was less likely to be included in our analyses because this was largely out of the range of the frozen season; within the frozen season, 95.3% of the 25-km pixels were on average frozen (Fig. S5).

To combine snow cover, frozen status, and frozen season, we extracted pixel values of different layers at the MODIS spatial resolution of 500 m. Specifically, we first determined the coordinates of pixel centers on the snow cover layer (fine resolution). Second, we transformed them into the coordinates under the coordinate systems of other data layers for freeze/thaw status and the start and end of the frozen season. Third, we extracted the freeze/thaw status and frozen season information (the start and end of the frozen season) from the pixel where each transformed coordinate fell. Finally, we checked if these extracted attributes met the criteria of D_{ws} and D_{wos}. We derived global D_{ws} and D_{wos} at 500-m spatial resolution from 2000 to 2012, and stored the data in a sinusoidal map projection for each MODIS tile. We did not calculate D_{ws} and D_{wos} for the non-cold constraint, permanent ice, non-vegetated, and urban areas in the MEaSUREs Freeze/Thaw data for which no freeze/thaw data were available.

We quantified global patterns of frozen ground with and without snow by calculating the mean and coefficient of variation (CV) of D_{ws} and D_{wos} for each pixel. We summarized the mean and CV of D_{ws} and D_{wos} for each one-degree interval of latitude and used local polynomial regression fitting (LOESS) to smooth these variables across latitude. LOESS curve fitting is a local regression model that fits a straight line or a polynomial curve in the locality of a given x value, weighting each of the (x_i, y_i) pairs according to the distance of x_i to x. It requires decisions to be made regarding the weights, the bandwidth around each point x, and the parametric functions to be fitted (Cleveland and Loader, 1996). Here, we carried out unweighted fit using a bandwidth of 75% of points and set the overall degree of the locally fitted polynomial to 2.

2.3. Accuracy assessment

For our accuracy assessment, we used the Global Historical Climatology Network (GHCN) data (Menne et al., 2012) to evaluate our remote sensing-derived D_{ws} and D_{wos}. We examined snow depth records for all stations of the GHCN data globally, and selected the stations with complete daily snow depth records from 2000 to 2012. Most stations that met the criteria were in North America with only a few stations in the Netherlands and Germans. Given this, we decided to focus our accuracy assessment on all 731 stations within North America in order to cover different land-cover types and elevational gradients. For each station, we extracted daily frozen/thawed status from the MEaSUREs Freeze/Thaw data records, and frozen season information from 2000 to 2012. We calculated D_{ws} and D_{wos} in the same way as above, but replaced the input MODIS snow cover with station-based snow depth. We extracted land-cover type for each station and each year from 2000 to 2012 from the MODIS land cover product of the corresponding year (because the MODIS land cover product started from 2001, we extracted the land-cover type for 2000 from MODIS land cover product of 2001). We made comparisons between remote sensing-based and station-based by calculating root-mean-square error (RMSE), linear regression slope (slope), and correlation coefficient (R), and summarized results by three land-cover types and four elevation levels (divided based on quantiles).

3. Results

3.1. Accuracy of D_{ws} and D_{wos}

D_{ws} values derived from the MODIS snow cover product were highly consistent with those using station-based snow depth data (RMSE = 18; Slope = 0.87; R = 0.96) (Fig. 2a). The accuracy of D_{ws} differed slightly among three main land-cover classes and among elevation (Table 1). In croplands, D_{ws} had the lowest RMSE and the slope closest to 1 (RMSE = 13; Slope = 0.93; R = 0.96), indicating the highest accuracy. In contrast, D_{ws} of forests had the lowest accuracy with the highest RMSE and the slope farthest from 1 (RMSE = 24; Slope = 0.83; R = 0.94). D_{ws} estimates at elevations of 250–500 m had higher accuracy as indicated by the lowest RMSE and the slope closer to 1 (RMSE = 15; Slope = 0.87; R = 0.94). In contrast, the estimates at elevations > 1500 m had lower accuracy as indicated by the highest

Table 2
Correlation coefficients, linear regression slopes, and root-mean-square errors between station-based D_{wos} and remote sensing-based D_{wos} by land cover classes and elevation levels.

	Land cover class			Elevation			
	Forest	Grassland	Cropland	<=250 m	250– 500 m	500– 1500 m	>1500 m
R	0.87	0.95	0.91	0.88	0.91	0.93	0.89
Slope	0.82	0.89	0.92	0.83	0.95	0.91	0.81
RMSE	22	16	13	17	15	16	20

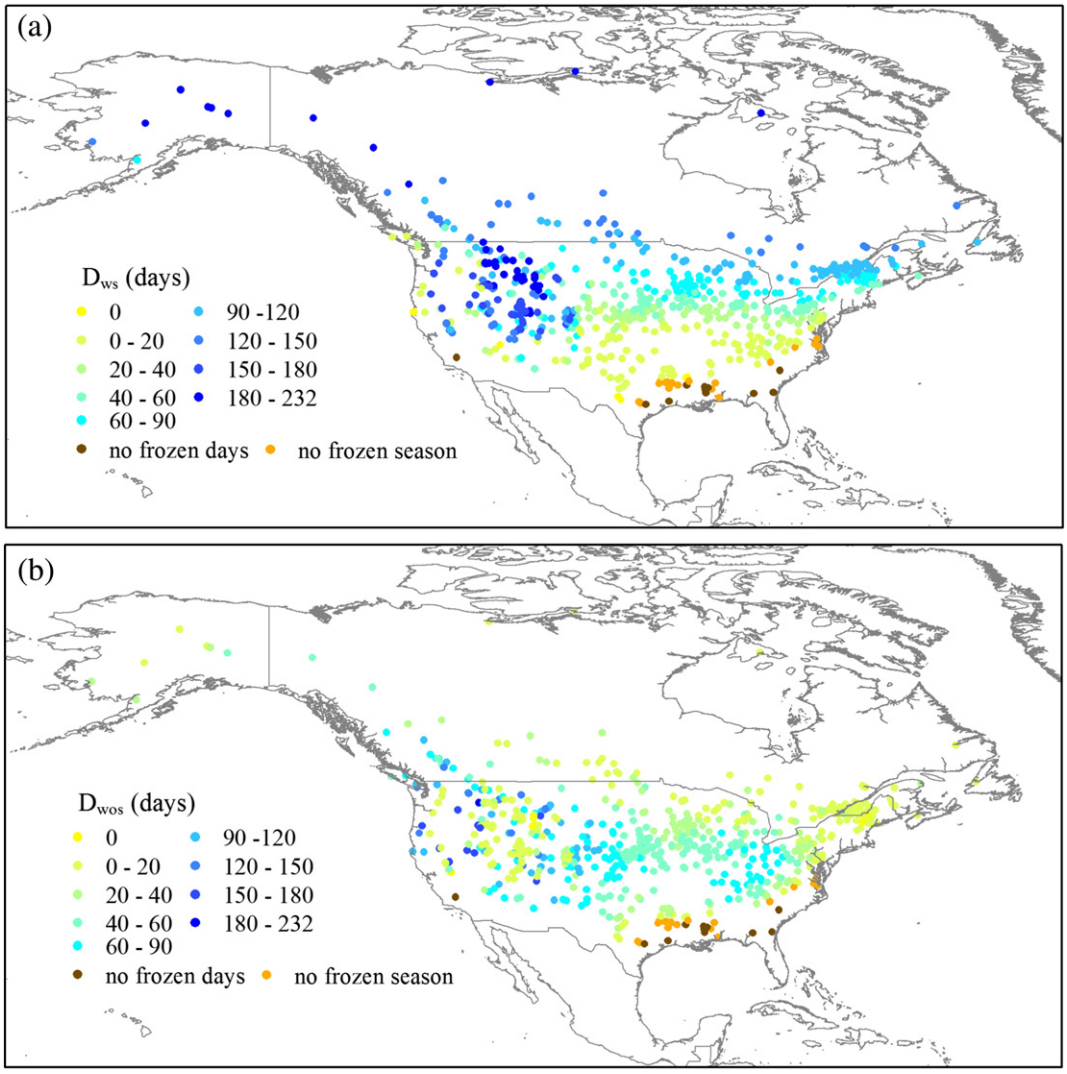

Fig. 3. Spatial patterns for 2000–2012 of (a) the mean duration of snow-covered frozen ground (D_{ws}) and (b) the mean duration of snow-free frozen ground (D_{wos}).

RMSE and the slope farther from 1 (RMSE = 21; Slope = 0.82; R = 0.94).

D_{wos} values derived from the MODIS snow cover product also showed high accuracy when assessed using station-based D_{wos} estimates (RMSE = 17; Slope = 0.88; R = 0.91) (Fig. 2b), but accuracy varied slightly by land-cover classes and elevation (Table 2). D_{wos} of croplands had higher accuracy as indicated by the lowest RMSE and the slope closer to 1 (RMSE = 13; Slope = 0.92; R = 0.91). In contrast, D_{wos} of forests had the lowest accuracy with the highest RMSE and the slope farthest from 1 (RMSE = 22; Slope = 0.82; R = 0.87). The accuracy for D_{wos} estimates at elevations of 250–500 m were highest with the lowest RMSE and the slope closest to 1 (RMSE = 15; Slope = 0.95; R = 0.91). By comparison, D_{wos} estimates at elevations > 1500 m had the lowest accuracy (RMSE = 20; Slope = 0.81; R = 0.89).

In addition to these overall summary statistics, we made maps of the spatial patterns of mean D_{ws} and D_{wos} according to station-based snow depth records (2000 − 2011) (Fig. 3a, b). Spatial patterns of D_{ws} and D_{wos} from station-based data were generally consistent with those derived from remotely sensed snow cover products (see below).

3.2. Global patterns of mean D_{ws} and D_{wos}

Snow-covered ground occurred mainly in the Northern Hemisphere (Fig. 4a). Of the global area with more than one day of snow-covered ground, the Northern Hemisphere accounted for 97%, and of the global area with >10 days of snow-covered ground, the Northern Hemisphere accounted for 99%. The global pattern of mean D_{ws} changed with latitude and topography (Fig. 4a). Spatially, D_{ws} became longer as latitude increased. Areas with long D_{ws} occurred mainly in mountainous regions at high altitude (including the Rocky Mountains, the Southern Andes Mountains, and the Tibetan Plateau) and at high latitudes (including Canada, Russia, Kazakhstan, and Mongolia). Shorter D_{ws} occurred in most cold-constrained areas of the Southern Hemisphere, and at middle and low latitude of the Northern Hemisphere (including the contiguous US, the Western Europe, and China). Overall, global patterns of mean D_{ws} are similar to those of the length of the frozen season, which indicates that D_{ws} becomes longer with increasing frozen season duration (Fig. 4a and b).

Fig. 4. Global patterns for 2000–2012 of (a) the mean duration of snow-covered frozen ground (D_{ws}), (b) the mean length of the frozen season, and (c) the mean duration of snow-free frozen ground (D_{wos}). No frozen season was assigned to pixels for which the start or the end of the frozen season was not detected in any year. No frozen days was assigned to pixels that had no frozen or transitional status in any year. Gray areas were excluded because they are in darkness for extended periods in winter. The white areas correspond to non-cold constraint, permanent ice, non-vegetated, or urban areas in the MEaSUREs Freeze/Thaw data for which no freeze/thaw data were available.

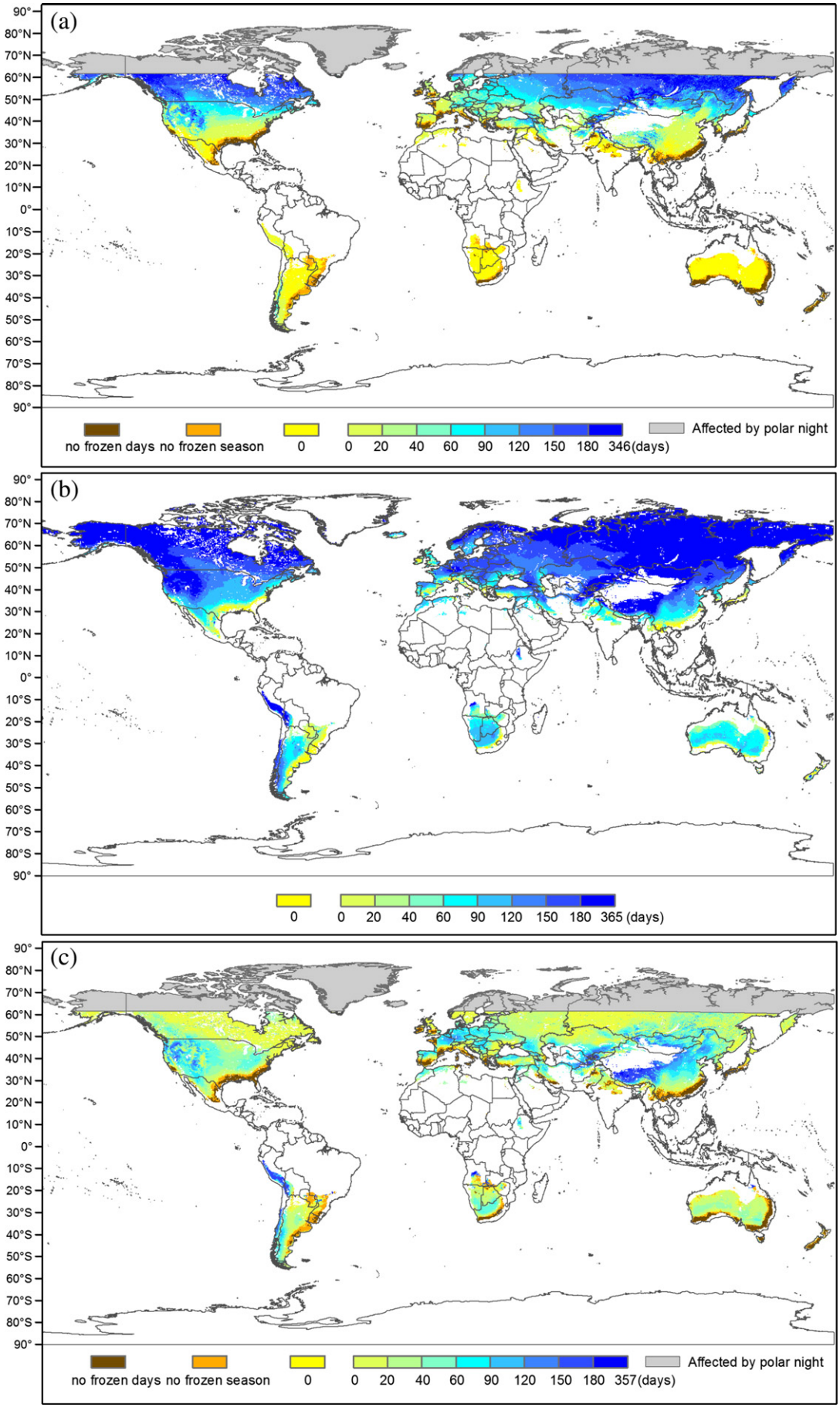
(a)
90°
80°N
70°N
60°N
50°N
40°N
30°N
20°N
10°N
0°
10°S
20°S
30°S
40°S
50°S
60°S
70°S
80°S
90°
no frozen days
no frozen season
0
0 20 40 60 90 120 150 180 346(days)
Affected by polar night
(b)
0
0 20 40 60 90 120 150 180 365 (days)
(c)
no frozen days
no frozen season
0
0 20 40 60 90 120 150 180 357(days)
Affected by polar night

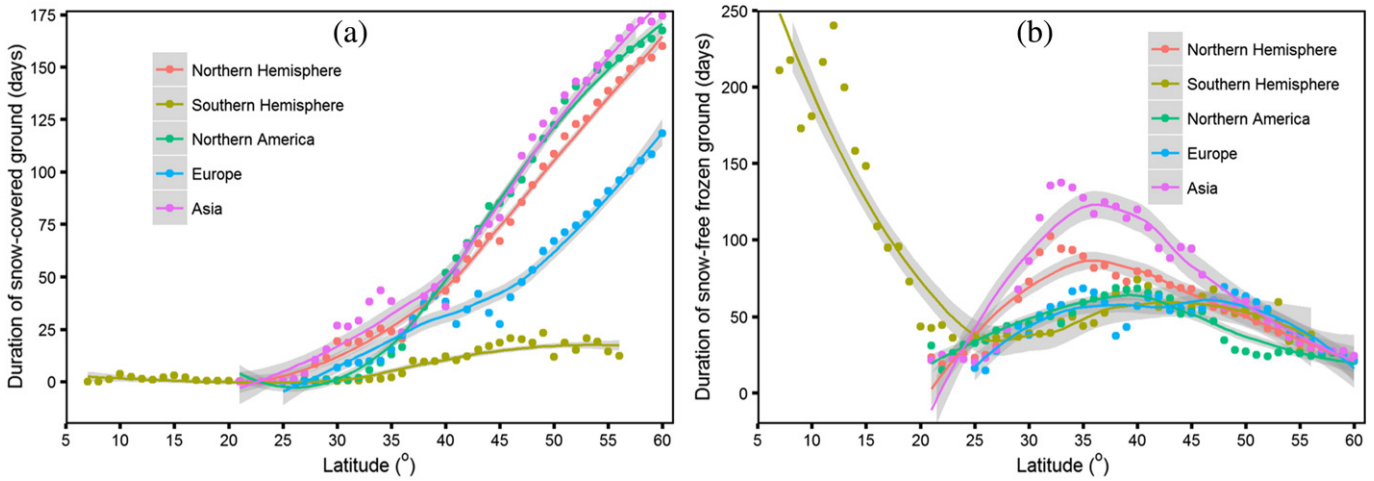

Fig. 5. Changes in (a) the duration of snow-covered ground, D_{ws}, and (b) the duration of snow-free frozen ground, D_{wos}, with latitude. We smoothed the data using the local polynomial regression fitting (LOESS) method, and gray bands represent 95% confidence intervals.

In contrast to D_{ws}, mean D_{wos} did not change monotonically with latitude (Fig. 4c): middle latitudes showed longer D_{wos}, even though the frozen season was shorter than at high latitudes. For example, we found long D_{wos} in the central contiguous US, Western Europe, northern China, and Mongolia. The high-latitude regions to the north (Canada, Russia, and Kazakhstan) had shorter D_{wos}. We also found shorter D_{wos} at low latitudes adjacent to areas with no evident frozen season (Fig. 4c).

We averaged mean D_{ws} and D_{wos} across one-degree latitudinal bands (Fig. 5). In both Northern and Southern Hemispheres, D_{ws} increased with latitude, but the rate of increase was much lower in the Southern Hemisphere (Fig. 5a). The increase of D_{ws} with latitude in North America was similar to that in Asia. In contrast, the slope of D_{ws} in Europe was relatively shallow; presumably, this is because winter in Europe is mild due to its temperate and maritime climate. This made D_{ws} shorter in Europe than in North America and Asia at the same latitude. In contrast to D_{ws}, D_{wos} was longest at 35–40°N in the Northern Hemisphere, decreasing both northward and southward (Fig. 5b). We found similar hump-shaped patterns with latitude in all northern continents, but the peak D_{wos} at middle latitudes (about 35–40°N) in Asia was much longer than in North America and Europe (Fig. 5b). In the Southern Hemisphere, D_{wos} decreased with latitude to 20–25°S. Overall, the change in D_{ws} and D_{wos} in the Southern Hemisphere depended mainly on the snow cover and frozen ground distribution in the Andes mountains, with longer D_{wos} towards the Equator and longer D_{ws} towards the south.

3.3. Global pattern of D_{ws} / (D_{ws} + D_{wos})

To derive a synoptic measure of the relative length of time frozen ground is covered by snow, we computed $100 * D_{ws} / (D_{ws} + D_{wos})$, and we refer to this as the D_{ws} percentage. While the D_{ws} reflects the absolute number of days of snow cover within the frozen season, the percentage indicates the duration of snow cover relative to the duration of the frozen period. The same D_{ws} values could correspond to different percentages, and vice versa. Moreover, compared to D_{ws} the percentage reflects whether snow was persistent or ephemeral on the ground. We found a zone in both North America and Eurasia where the gradient of percentages changed rapidly from 20% to 90% (Fig. 6). Spatially, D_{ws} percentage changed consistently with latitude (Fig. 6). The areas with higher D_{ws} percentage were mainly distributed at high latitudes (e.g., Canada and Russia) and in mountainous areas (e.g., the Rocky Mountains and the southern Andes Mountains). In contrast, the areas at middle and low latitudes had relatively lower D_{ws} percentage, which included most cold-constrained areas of the Southern Hemisphere, the contiguous US (except for the western mountainous regions), Western Europe, and China.

We averaged D_{ws} percentage in one-degree latitudinal bands (Fig. 7). In the Northern Hemisphere, D_{ws} percentage increased fastest at middle latitudes (Fig. 7). In the Southern Hemisphere, D_{ws} percentage was lower between 7 and 30°S, and then started to increase further south with a lower slope than in the Northern Hemisphere. Patterns of D_{ws} percentage were similar among continents in the Northern Hemisphere, although D_{ws} percentages in North America and Asia were higher than those in Europe above 43°N.

3.4. Interannual variation in D_{ws} and D_{wos}

Interannual variation in D_{ws} and D_{wos} is important for organisms, especially species depending on the subnivium (Pauli et al., 2013; Petty et al., 2015; Williams et al., 2014). If climate warming leads to a reduction of snow cover, resulting in exposure to lower air temperatures, this may lead to an increasing frequency of freeze-thaw cycles and higher risk of ice encasement (Bale and Hayward, 2010). The CV is the standard deviation divided by the mean; dividing by the mean removes the inevitable dependence of the standard deviation of D_{ws} and D_{wos} on the duration of frozen days with and without snow cover, respectively. Thus, CV measures the relative interannual variation in D_{ws} and D_{wos} among years, with lower values indicating less variability.

Interannual variation in D_{ws} decreased with latitude (Fig. 8a). Areas with low interannual variation in D_{ws} occurred mainly in Canada, Russia, Kazakhstan, and some mountainous regions (e.g., Rocky Mountains), while the areas at middle and low latitudes, including the contiguous US, the Western Europe, China and Mongolia, had greater interannual variation (Fig. 8a). Interestingly, we found the highest interannual variation in D_{ws} in the Tibetan Plateau and Andes Mountains. In contrast, higher interannual variation in D_{wos} was observed at high latitudes of North America (except for the western mountainous areas), Russia, and Kazakhstan, while the vast middle-latitude areas had lower interannual variation in D_{wos}, which included the contiguous US, Western Europe, and China (Fig. 8b).

We averaged the CV in D_{ws} and D_{wos} in one-degree latitudinal bands (Fig. 9). In the Northern Hemisphere, the CV of D_{ws} diminished with latitude, and the rate of decrease was higher at low latitudes (Fig. 9a). However, we found a nonlinear relationship between the CV of D_{wos} and latitude in the Northern Hemisphere, which was characterized by a decreasing trend below 33°N and an increasing trend further north (Fig. 9b). The CV of D_{wos} in Asia was higher at low latitudes than in North America, but lower at high latitudes. However, the CV of D_{wos} in Europe did not show the nonlinear relationship with latitude. In the

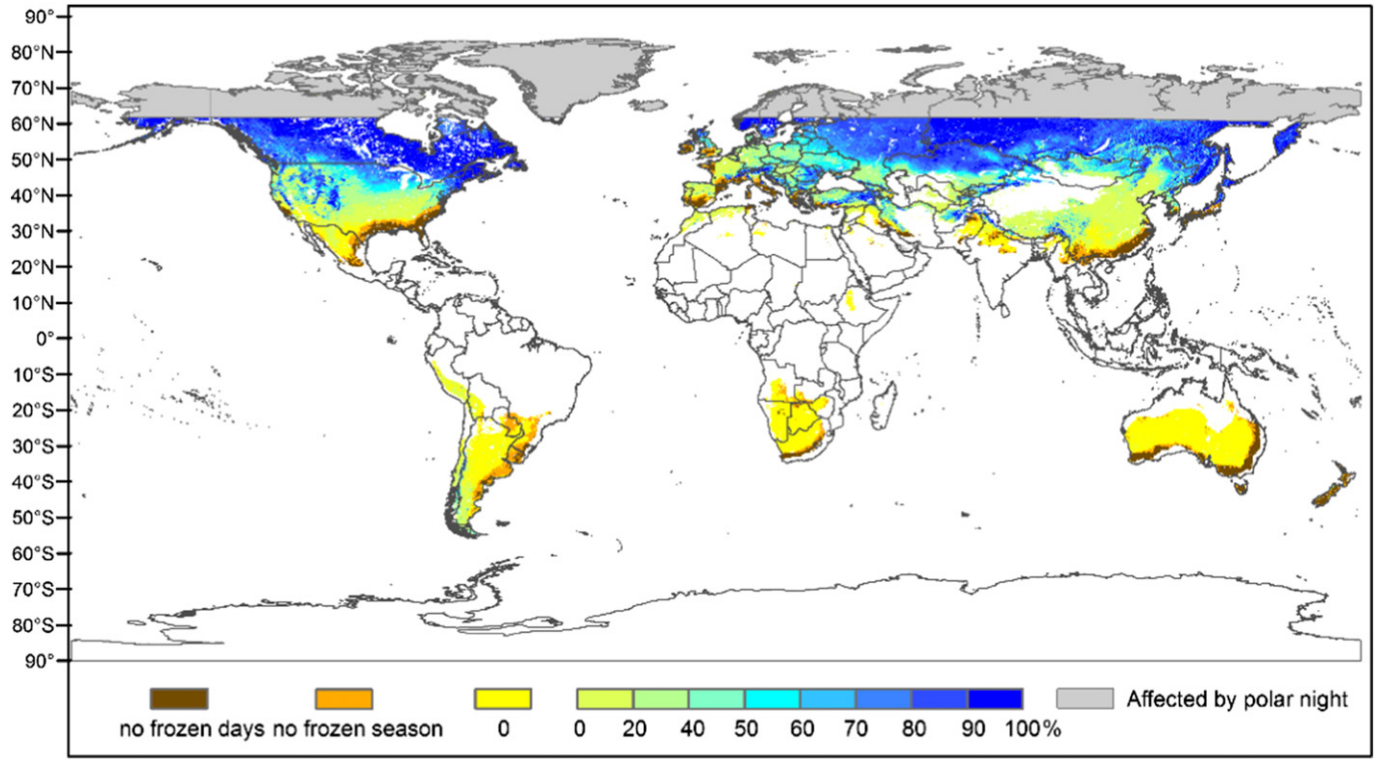

Fig. 6. Global pattern of D_{ws} percentage, $100 * D_{ws} / (D_{ws} + D_{wos})$.

Southern Hemisphere, the CV of both D_{ws} and D_{wos} decreased with latitude.

4. Discussion

We developed a new global dataset from 2000 to 2012 that captures the duration of snow-covered ground (D_{ws}) and snow-free frozen ground (D_{wos}) by combining the MODIS Snow Cover product and the NASA MEaSUREs Freeze/Thaw dataset from SSM/I and SSMIS. We calculated both metrics annually based on the estimated frozen season on a per-pixel basis. We generated our new dataset at the MODIS spatial resolution of 500 m rather than at the spatial resolution of the freeze/thaw data (25 km), because the landscape frozen/thawed status was relatively homogenous within the 25-km grid, as inferred from analyses of Daymet data. We analyzed global patterns of mean D_{ws} and D_{wos} and their interannual variation (2000–2012). As expected, we found that areas at high latitudes had longer D_{ws}. Counter-intuitively though, areas at middle latitudes had longer D_{wos}, even though the frozen season was shorter than at high latitudes. Our research is useful for understanding the duration and condition of the subnivium, which determines the local microclimate inhabited by many organisms in winter. Not only is this valuable information for understanding present distributions and fluctuations in plant, animal, and microbe populations, it also provides a baseline to assess the effects of future climate change on organisms that overwinter.

We quantified spatial patterns of mean D_{ws} and D_{wos}, and their variation with latitude. We found that the spatial pattern of D_{ws} coincided with that of the length of the frozen season, with D_{ws} increasing with the duration of the frozen season. Longer D_{ws} at high-latitudes resulted from long frozen seasons and lower air temperatures. In general, the duration of frozen ground correlates positively with the extent of snow cover throughout the year, and in a given season, especially at high latitudes (Kim et al., 2015). Air temperatures could also influence D_{ws} by determining whether and how long snow cover stays on the ground. Increasing temperatures may reduce the duration of snow-covered frozen ground causing earlier spring thawing or later fall freezing, and by shortening the persistence of snow cover on the ground (Choi et al., 2010; Kim et al., 2012; Peng et al., 2013). In contrast to D_{ws}, we found longer duration of snow-free frozen ground at middle latitudes, even though the frozen season was shorter there than at high latitudes. This pattern is highlighted by the hump-shaped relationship between the D_{wos} and latitude (Fig. 5b). At middle latitudes, longer frozen season duration coincides with low temperate and dry climate zones that promote less precipitation in winter and are not favorable for snow persistence, leading to low or negative correlations between frozen season and snow-cover duration (Kim et al., 2015). Therefore, vast areas at middle latitudes had a longer absence of the subnivium while the ground was frozen (Brown and DeGaetano, 2011; Pauli et al., 2013; Petty et al., 2015). For many organisms that rely on the subnivium, this implies that middle latitudes might be functionally colder than either more southerly or more northerly latitudes.

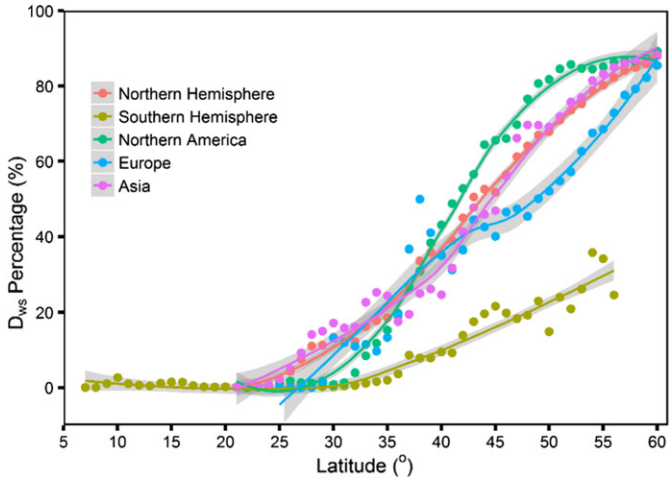

Fig. 7. Changes in the D_{ws} percentage with latitude. We smoothed the data using the LOESS method, and gray bands represent 95% confidence intervals.

We quantified global patterns of temporal variation in D_{ws} and D_{wos}. We found that temporal variation in D_{ws} was less at high latitudes, because temperatures within the frozen season at high latitudes were cold enough to maintain snow cover. In contrast, mid- and low-latitude areas had greater temporal variation in D_{ws} due to the longer period of transitional frozen/thawed state that made snow cover less stable. Prior research showed that mid- and low-latitude areas have longer annual snowmelt periods and greater annual fluctuations in the length of the snow season (i.e., the interval between the first appearance and the last disappearance of snow) (Choi et al., 2010; Kim et al., 2015). Although D_{ws} was longer and stable at high latitudes, D_{wos} had greatest temporal variation at high latitudes.

For organisms that rely on the subnivium, D_{wos} gives an indicator of the number of days when cold stress may be particularly severe. Therefore, D_{wos} may be a key measure of the potential effects of future climate

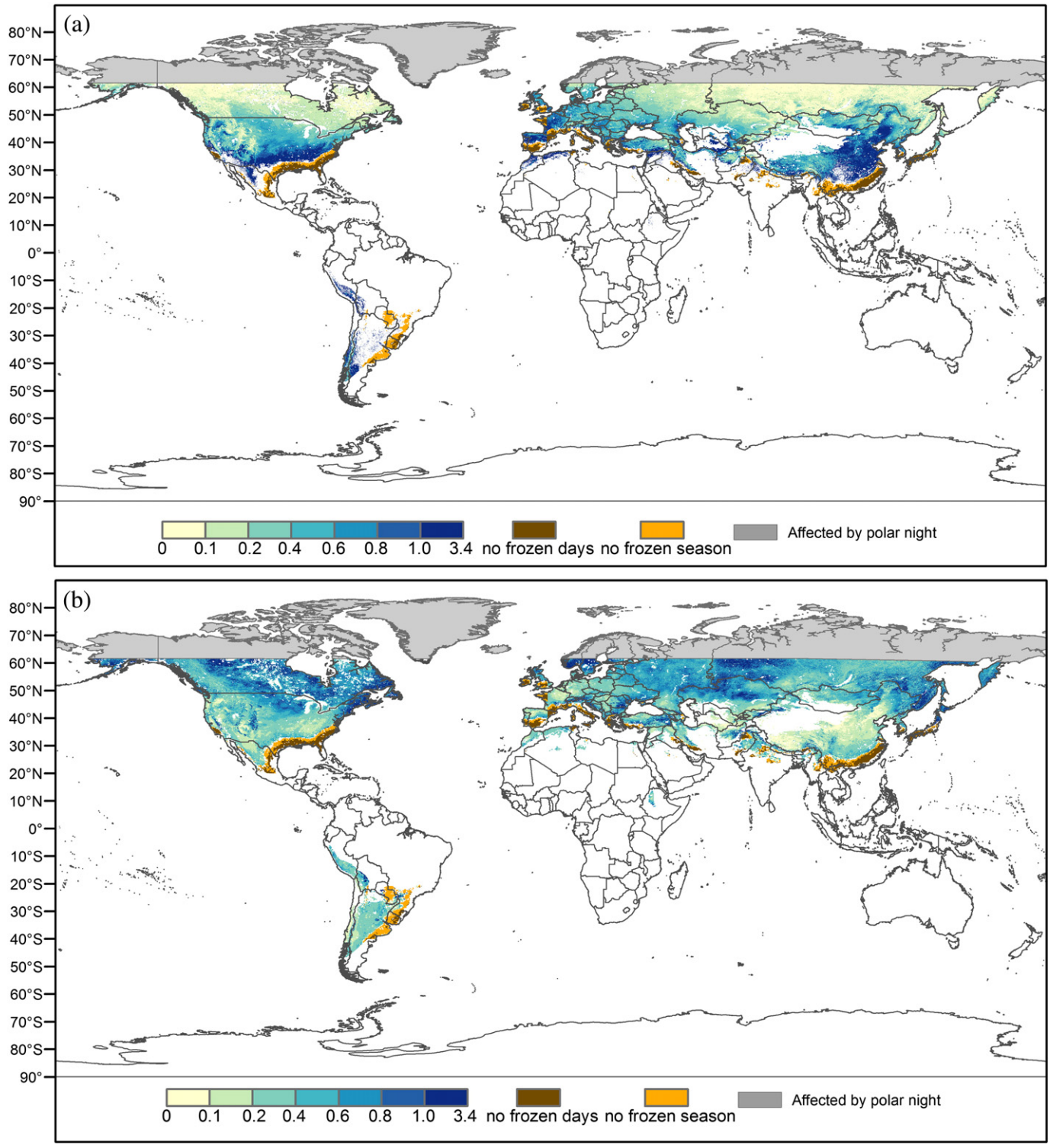

Fig. 8. Global pattern of the temporal variation (CV) for (a) the duration of snow-covered ground (D_{ws}) from 2000 to 2012 and (b) the duration of snow-free frozen days (D_{wos}) from 2000 to 2012.

change on these overwintering organisms. However, we did not perform a trend analysis of our data because our time series is too short, having only 12 years. Other research, though, has already found substantial changes in snowmelt period, frozen ground duration and snow cover duration in high-latitude areas (Kim et al., 2015; Peng et al., 2013), and current forecasts predict greater rates of global warming at higher latitudes than towards the Equator (IPCC, 2014). This warming may though increase cold stress at high latitudes if it increases mean D_{wos} towards values currently found at mid latitudes (Fig. 5). High latitudes are currently experiencing the greatest interannual variation in D_{wos} (Fig. 7), and if this high variation is maintained at the same time as mean D_{wos} increases, then organisms that rely on the subnivium may be subject to particular cold stress, with high and highly variable duration of frozen ground with no snow cover. The high Arctic, however, is also forecast to have increased precipitation with global warming (IPCC, 2014), and if this precipitation adds to snow cover, then the effects of increasing temperature on D_{wos} could be mitigated.

Several potential sources of error may have affected the accuracy of our dataset. MODIS sensors detect solar radiation reflected from targets on the ground. Daily MODIS images are often contaminated by cloud cover, which is why we chose the 8-day composite MODIS snow cover product, which provides the maximum snow extent at 8-day intervals. By using this dataset for our calculations, we assumed that all eight days would be covered by snow if a pixel was classified as 'snow'. However, this assumption may not always be true, especially at low latitudes, and this may have caused overestimates of D_{ws}. We reduced this potential bias by constraining the calculation of D_{ws} to days within our pre-defined frozen season. Furthermore, even in the 8-day composite MODIS snow cover product some pixels were cloudy, and these could lead to underestimates of D_{ws}, which is why we interpolated the cloud pixels using their neighbors across space and time for only winter months. In addition, the accuracy of MODIS snow cover is influenced by varied snow depth, land-cover types, and the number of days used for compositing (Hall and Riggs, 2007; Liang et al., 2008; Pu et al., 2007), all of which might have affected our estimates of D_{ws} and D_{wos}. Finally, because the current NASA MEaSUREs Freeze/Thaw records stopped in 2012, we could only generate D_{ws} and D_{wos} for the period 2000–2012. This 13-year time period is too short to investigate long-term trends in the durations of frozen days with and without snow cover.

The freeze/thaw data product determines freeze/thaw status by comparing a spatial and seasonal scale factor derived from brightness temperatures (T_b) with dynamic thresholds on yearly and cell-by-cell bases (Kim et al., 2011). However, the empirical algorithm derived from the linear relationships between Tb–based scale factors and surface temperatures does not take into account the different contributions to the microwave signal from soil, vegetation, snow, and so forth. Hence, the FT product reflects landscape FT rather than only soil FT. In boreal forests, the uncertainties in identifying soil FT might be particularly high because of the complex continuum of soil, snow, and forests (Roy et al., 2015; Roy et al., 2016). For example, in boreal forests where the deep organic soil is saturated with water, the delay between forest freezing and soil freezing might cause inaccurate freeze/thaw status. We also caution that the mapping of frozen/thawed status is much more complex when ground is covered by snow (Jones et al., 2007; Rawlins et al., 2005). Thus, the frozen status for snow-cover ground might reflect the conditions of snow rather than soil depending on the influence of snow pack's wetness, depth, density, crystal structure on brightness temperatures (Mcdonald and Kimball, 2005). For example, the temperature retrievals from microwave satellites correspond more closely to minimum daily air temperatures and MODIS land surface temperatures than soil temperatures for snow-cover areas (Jones et al., 2007). However, the subnivium depends mainly on whether the ground is covered by snow or not. Whether or not the ground is frozen only matters where there is no snow cover. Therefore, even though some of the retrievals may present frozen/thawed status of the snow pack instead of the soils, we are not overly concerned about this, because our calculated D_{ws}, which is defined as the number of days when ground was covered by snow and classified as frozen, is still a good measure of the subnivium.

5. Conclusions

Our research characterized global patterns of snow-covered and snow-free frozen ground, which can be useful indicators of the effects of cold temperatures on organisms. Frozen ground without a buffering snow cover may expose soil systems to more-extreme low temperatures, damage vegetation, and reduce winter soil decomposition and respiration processes (Isard and Schaetzl, 2007; Kim et al., 2015; Williams et al., 2014). Indeed, organisms from very cold and snowy regions are frequently less cold-tolerant than those from regions with a shallower and less-persistent snowpack (Williams et al., 2014). Similar to the complex mechanisms during the growing season, the frozen season is characterized by complicated interactions among climate, land surface, and ecosystems (Williams et al., 2014). Winter climate change impacts land surface status by altering snow cover (e.g., extent, depth, and snowmelt), soil freeze/thaw cycles, and lake and river ice (Fountain et al., 2012; Kim et al., 2012), and in turn, these changes give positive or negative feedbacks to climate (Chapin et al., 2008; Euskirchen et al., 2007; Peng et al., 2013). The combined climate and

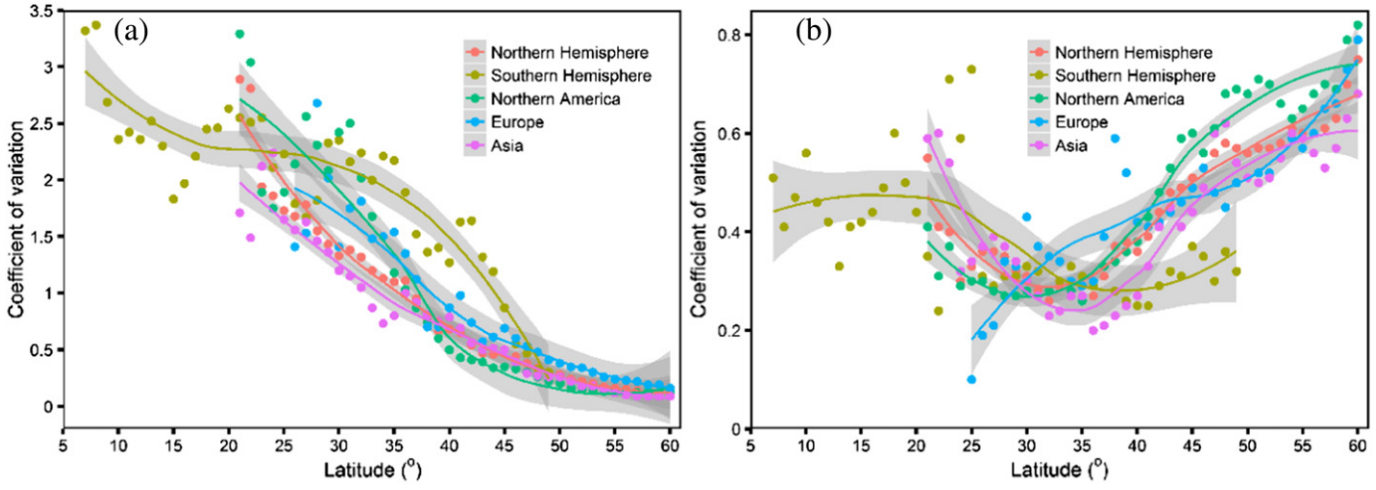

Fig. 9. Changes of (a) the coefficient of variation (CV) for D_{ws} and (b) the CV for D_{wos} with latitude. We smoothed the data using the LOESS method, and gray bands represent 95% confidence intervals.

land surface changes have strong influence on organisms, their biophysical conditions, and underlying biogeochemical processes (Kreyling, 2010; Makoto et al., 2013; Starr and Oberbauer, 2003). Our remote sensing-based data at medium spatial resolution offer important inputs for both ecological and biogeochemical models to understand organism-environment interactions at broad scales, thereby providing a baseline to assess the effects of future climate change on ecosystems.

We integrated two satellite-based datasets, the MODIS snow cover product and NASA MEaSUREs Freeze/Thaw dataset from the SSM/I and SSMIS, and developed a new global dataset at a spatial resolution of 500 m from 2000 to 2012 that captures global patterns of the duration of snow-covered ground (D_{ws}) and snow-free frozen ground (D_{wos}). Generally, D_{ws} was longer at higher latitudes, which coincided with the spatial pattern of the length of the frozen season. Areas at middle latitudes had longer D_{wos}, even though the frozen season was shorter. Furthermore, D_{wos} had relatively higher temporal variation at high latitudes. Therefore, vast middle-latitude areas may be functionally colder for organisms that use the subnivium, because soil surface temperatures when uncovered by snow may be very low. Global warming may result in a counter-intuitive trend of large areas, especially at high latitudes, becoming functionally colder as snow cover diminishes, which has important consequences for overwintering organisms.

Acknowledgments

We gratefully acknowledge support for this work by NSF's Dimensions of Biodiversity program (No. 1240804), and by NASA's Biodiversity and Ecological Forecasting program (NNX14AP07G). Two anonymous reviewers provided very constructive feedback that greatly improved the manuscript, and we thank them for their suggestions.

Appendix A. Supplementary data

Supplementary data to this article can be found online at http://dx.doi.org/10.1016/j.rse.2017.01.020.

References

Aitchison, C.W., 2001. The effect of snow cover on small animals. In: Jones, H.G., Pomeroy, J.W., Walker, D.A., Hoham, R.W. (Eds.), Snow Ecology: An Interdisciplinary Examination of Snow Covered Ecosystems. Cambridge University Press, pp. 229–265.
Bale, J.S., Hayward, S.A.L., 2010. Insect overwintering in a changing climate. J. Exp. Biol. 213 (6), 980–994.
Brown, P.J., DeGaetano, A.T., 2011. A paradox of cooling winter soil surface temperatures in a warming northeastern United States. Agric. For. Meteorol. 151 (7), 947–956.
Campbell, J.J.L., Mitchell, M.J.M., Groffman, P.M.P., Christenson, L.M., Hardy, J.P., 2005. Winter in northeastern North America: a critical period for ecological processes. Front. Ecol. Environ. 3 (6), 314–322.
Chapin, F.S., Randerson, J.T., McGuire, A.D., Foley, J.A., Field, C.B., 2008. Changing feedbacks in the climate-biosphere system. Front. Ecol. Environ. 6 (6), 313–320.
Choi, G., Robinson, D.A., Kang, S., 2010. Changing northern hemisphere snow seasons. J. Clim. 23 (19), 5305–5310.
Cleveland, W.S., Loader, C.L., 1996. Smoothing by local regression: principles and methods. In: Haerdle, W., Schimek, M.G. (Eds.), Statistical Theory and Computational Aspects of Smoothing. Springer, Berlin, Heidelberg, NY, pp. 10–49.
Decker, K.L.M., Wang, D., Waite, C., Scherbatskoy, T., 2001. Snow removal and ambient air temperature effects on forest soil temperatures in northern Vermont. America Journal]–>Soil Sci. Soc. Am. J. 67, 1234–1243.
Déry, S.J., Brown, R.D., 2007. Recent Northern Hemisphere snow cover extent trends and implications for the snow-albedo feedback. Geophys. Res. Lett. 34 (22), 2–7.
Dye, D.G., 2002. Variability and trends in the annual snow-cover cycle in Northern Hemisphere land areas, 1972–2000. Hydrol. Process. 16 (15), 3065–3077.
Estilow, T.W., Young, A.H., Robinson, D.A., 2014. A long-term Northern Hemisphere snow cover extent data record for climate studies and monitoring. Earth System Science Data 7, 669–691.
Euskirchen, E.S., Mcguire, A.D., Chapin, F.S., 2007. Energy feedbacks of northern high-latitude ecosystems to the climate system due to reduced snow cover during 20th century warming. Glob. Chang. Biol. 13 (11), 2425–2438.
Fountain, A.G., Campbell, J.L., Schuur, E.A.G., Stammerjohn, S.E., Williams, M.W., Ducklow, H.W., 2012. The disappearing cryosphere: impacts and ecosystem responses to rapid cryosphere loss. Bioscience 62 (4), 405–415.
Frei, A., Tedesco, M., Lee, S., Foster, J., Hall, D.K., Kelly, R., Robinson, D.A., 2012. A review of global satellite-derived snow products. Adv. Space Res. 50 (8), 1007–1029.
Hall, D.K., Riggs, G.A., 2007. Accuracy assessment of the MODIS snow products. Hydrol. Process. 21, 2267–2274.
Hall, D.K., Riggs, G.A., Salomonson, V.V., DiGirolamo, N.E., Bayr, K.J., 2002. MODIS snow-cover products. Remote Sens. Environ. 83 (1–2), 181–194.
IPCC, 2014. In: Core Writing Team, Pachauri, R.K., Meyer, L.A. (Eds.), Climate Change 2014: Synthesis Report. Contribution of Working Groups I, II and III to the Fifth Assessment Report of the Intergovernmental Panel on Climate Change. IPCC, Geneva, Switzerland (151 pp).
Isard, S.A., Schaetzl, R.J., 2007. Soils cool as climate warms in the Great Lakes Region: 1951–2000. American Geographers]–>Ann. Assoc. Am. Geogr. 97, 467–476.
Jones, H.G., 1999. The ecology of snow-covered systems: a brief overview of nutrient cycling and life in the cold. Hydrol. Process. 13, 2135–2147.
Jones, L.A., Member, S., Kimball, J.S., Mcdonald, K.C., Member, S., Chan, S.T.K., Njoku, E.G., Oechel, W.C., 2007. Satellite microwave remote sensing of boreal and Arctic soil temperatures from AMSR-E. IEEE Trans. Geosci. Remote Sens. 45 (7), 2004–2018.
Kim, Y., Kimball, J.S., McDonald, K.C., Glassy, J., 2011. Developing a global data record of daily landscape freeze/thaw status using satellite passive microwave remote sensing. IEEE Trans. Geosci. Remote Sens. 49 (3), 949–960.
Kim, Y., Kimball, J.S., Zhang, K., McDonald, K.C., 2012. Satellite detection of increasing Northern Hemisphere non-frozen seasons from 1979 to 2008: Implications for regional vegetation growth. Remote Sens. Environ. 121, 472–487.
Kim, Y., Kimball, J.S., Robinson, D.A., Derksen, C., 2015. New satellite climate data records indicate strong coupling between recent frozen season changes and snow cover over high northern latitudes. Environ. Res. Lett. 10 (8), 084004.
Klein, A.G., Barnett, A.C., 2003. Validation of daily MODIS snow cover maps of the Upper Rio Grande River Basin for the 2000–2001 snow year. Remote Sens. Environ. 86 (2), 162–176.
Kreyling, J., 2010. Winter climate change: a critical factor for temperate vegetation performance. Ecology 91 (7), 1939–1948.
Liang, T., Huang, X., Wu, C., Liu, X., Li, W., Guo, Z., Ren, J., 2008. An application of MODIS data to snow cover monitoring in a pastoral area: a case study in Northern Xinjiang, China. Remote Sens. Environ. 112 (4), 1514–1526.
Makoto, K., Kajimoto, T., Koyama, L., Kudo, G., Shibata, H., Yanai, Y., Cornelissen, J.H.C., 2013. Winter climate change in plant–soil systems: summary of recent findings and future perspectives. Ecol. Res. 29 (4), 593–606.
Mcdonald, K.C., Kimball, J.S., 2005. 53: estimation of surface freeze – thaw states using microwave sensors. In: Anderson, M.G. (Ed.), Encyclopedia of Hydrological Sciences. John Wiley & Sons, Inc., Hoboken, NJ, pp. 1–15.
Menne, M.J., Durre, I., Vose, R.S., Gleason, B.E., Houston, T.G., 2012. An overview of the global historical climatology network-daily database. J. Atmos. Ocean. Technol. 29, 897–910.
Pauli, J.N., Zuckerberg, B., Whiteman, J.P., Porter, W., 2013. The subnivium: a deteriorating seasonal refugium. Front. Ecol. Environ. 11 (5), 260–267.
Peng, S., Piao, S., Ciais, P., Friedlingstein, P., Zhou, L., Wang, T., 2013. Change in snow phenology and its potential feedback to temperature in the Northern Hemisphere over the last three decades. Environ. Res. Lett. 8, 014008.
Petty, S.K., Zuckerberg, B., Pauli, J.N., 2015. Winter conditions and land cover structure the subnivium, a seasonal refuge beneath the snow. PLoS One 10, e0127613.
Pu, Z., Xu, L., Salomonson, V.V., 2007. MODIS/Terra observed seasonal variations of snow cover over the Tibetan Plateau. Geophys. Res. Lett. 34 (6), 1–6.
Rawlins, M.A., Mcdonald, K.C., Frolking, S., Lammers, R.B., Fahnestock, M., Kimball, J.S., Vo, C.J., 2005. Remote sensing of snow thaw at the pan-Arctic scale using the SeaWinds scatterometer. J. Hydrol. *312*, 294–311.
Roy, A., Royer, A., Montpetit, B., Langlois, A., 2015. Microwave snow emission modeling of boreal forest environments. IGARSS2015, 26–31 July 2015, Milan, Italy, pp. 1–4.
Roy, A., Royer, A., St-jean-rondeau, O., Montpetit, B., Picard, G., Mavrovic, A., Marchand, N., Langlois, A., 2016. Microwave snow emission modeling uncertainties in boreal and subarctic environments. Cryosphere 10, 623–638.
Schimel, J.P., Bilbrough, C., Welker, J.M., 2004. Increased snow depth affects microbial activity and nitrogen mineralization in two Arctic tundra communities. Soil Biol. Biochem. 36 (2), 217–227.
Smith, N.V., Saatchi, S.S., Randerson, J.T., 2004. Trends in high northern latitude soil freeze and thaw cycles from 1988 to 2002. Journal of Geophysical Research D: Atmospheres 109, 1–14.
Starr, G., Oberbauer, S.F., 2003. Photosynthesis of arctic evergreens under snow: implications for tundra ecosystem carbon balance. Ecology 84 (6), 1415–1420.
Sullivan, P.F., Welker, J.M., Arens, S.J.T., Sveinbjo, B., 2008. Continuous estimates of CO_2 efflux from arctic and boreal soils during the snow-covered season in Alaska. J. Geophys. Res. 113, G04009. http://dx.doi.org/10.1029/2008JG000715.
Thornton, P.E., Thornton, M.M., Mayer, B.W., Wei, Y., Devarakonda, R., Vose, R.S., Cook, R.B., 2016. Daymet: Daily Surface Weather Data on a 1-km Grid for North America, Version 3. ORNL DAAC, Oak Ridge, Tennessee, USA. http://dx.doi.org/10.3334/ORNLDAAC/1328.
Williams, C.M., Henry, H.A.L., Sinclair, B.J., 2014. Cold truths: how winter drives responses of terrestrial organisms to climate change. Biol. Rev. 90, 214–235.
Xu, L., Myneni, R.B., Chapin III, F.S., Callaghan, T.V., Pinzon, J.E., Tucker, C.J., et al., 2013. Temperature and vegetation seasonality diminishment over northern lands. Nat. Clim. Chang. 3 (3), 581–586.
Zhang, K., Kimball, J.S., Kim, Y., McDonald, K.C., 2011. Changing freeze-thaw seasons in northern high latitudes and associated influences on evapotranspiration. Hydrol. Process. 25 (26), 4142–4151.